Available online at www.sciencedirect.com
ScienceDirect
Journal of Organometallic Chemistry 691 (2006) 4667–4675
Journal of Organometallic Chemistry
www.elsevier.com/locate/jorganchem

Stereodynamics and conformational equilibria in some chiral pseudo-octahedral tungsten crotyl complexes

Jack W. Faller *, Philip P. Fontaine

Department of Chemistry, Yale University, P.O. Box 208107, New Haven, CT 06520-8107, USA

Received 6 July 2006; received in revised form 28 July 2006; accepted 28 July 2006
Available online 12 August 2006

Abstract

The complexes $W(CO)_2(\eta^3$-crotyl)(diphos)X, where X = Cl and I, and $[W(CO)_3(\eta^3$-crotyl)(diphos)]SbF_6 were prepared and characterized. The solution dynamics were examined with low temperature NMR experiments, with focus on the effect of the crotyl ligand on controlling the chirality at the metal. A steric influence of halide was also observed which results in different conformational and configurational preferences for the crotyl group. The spontaneous resolution of the neutral complex $W(CO)_2(\eta^3$-crotyl)(diphos)Cl provides a route for obtaining optically active samples of these compounds. It was found that the conversion to the cationic tricarbonyl complex greatly increases the racemization barrier of the chiral center in the crotyl and also renders the η^3-ligand more susceptible to nucleophilic attack.

Keywords: Chiral induction; Crystallization-induced asymmetric transformation; Resolution

1. Introduction

Complexes of the type $M(CO)_2(\eta^3$-allyl)(diphos)X (M = Mo or W, X = halide) adopt a pseudo-octahedral geometry in which the arrangement of ligands about the metal center is chiral [1,2]. In cases where the allyl ligand is unsymmetrically substituted, such as crotyl, a stereogenic carbon center is also produced at the substituted terminus of the η^3 ligand. We have found that $Mo(CO)_2(\eta^3$-crotyl)(diphos)Cl (**1**) crystallizes as a conglomerate, where a given crystal contains a single enantiomer [3]. Thus, it is possible to manually separate the enantiomers and to obtain enantiomerically pure samples of this metal complex. Furthermore, the use of (*S*,*S*)-chiraphos in place of diphos results in the formation of only a single enantiomer upon slow crystallization, via a crystallization-induced asymmetric transformation [3]. Since **1** has been previously employed as a stoichiometric allylation reagent [4], and given the general utility of Mo [4–15] and W [9,11,16–20] compounds in allylic alkylation reactions, the ability to obtain these complexes in enantiopure form is promising in terms of use in asymmetric synthesis.

This class of complexes is fluxional [1,2,21,22], and so one needs to consider their solution dynamics in order to better understand their reactivity. Specifically, they exist as a pseudo-octahedral isomer in which one of the phosphorus atoms of the P–P chelate binds *trans* to the η^3-allyl group. This leaves an equatorial plane containing the two CO ligands, the halide ligand, and the other phosphorus atom. A trigonal twist rearrangement is operational that involves a rotation of the triangular face formed by the halide and the two phosphorus atoms relative to the face formed by the allyl and two CO groups (Fig. 1). It has been seen that this process occurs with a relatively low energy barrier (~8–12 kcal/mol), with the interconversion rates increasing with decreasing size of the halide (I < Br < Cl) [1,2,22].

We wish to report herein the results of a recent study on the solution dynamics of such complexes with an η^3-crotyl ligand. It was found that the unsymmetrical crotyl moiety exerts a strong control on the metal chirality. An

* Corresponding author. Fax: +1 203 432 6144.
E-mail address: jack.faller@yale.edu (J.W. Faller).

0022-328X/$ - see front matter © 2006 Elsevier B.V. All rights reserved.
doi:10.1016/j.jorganchem.2006.07.037

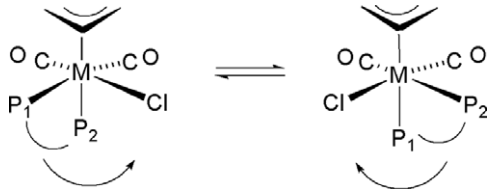

Fig. 1. Trigonal twist rearrangement.

interesting effect was also observed concerning the ability of the halide ligand to influence the *anti*/*syn* geometry of the η^3 ligand. Additionally, a cationic tricarbonyl analogue was prepared, and it was seen that for this complex the barrier to racemization of the η^3-crotyl ligand was greatly increased with respect to the neutral analogues.

2. Results and discussion

2.1. Variable temperature NMR of neutral complexes

Low temperature NMR experiments were used to probe the dynamics of these complexes. Since it has been observed that the trigonal twist rearrangement is slower for the tungsten complexes, $W(CO)_2(\eta^3$-allyl)(diphos)Cl (**2**) and $W(CO)_2(\eta^3$-crotyl)(diphos)Cl (**3**) were used for this study. Indeed, with these complexes low temperature limiting spectra could be obtained, making it possible to investigate the effects of the unsymmetrical crotyl ligand.

In the case of **2**, the room temperature $^{31}P\{^1H\}$ NMR shows a single resonance. This is a result of the averaging effect of the rearrangement process, which exchanges the two phosphorus atoms between two equivalent sites. Lowering the temperature causes the resonance to broaden until decoalescence at ~−40 °C, further cooling resulted in splitting into two resonances of equal intensity (Fig. 2). The low temperature limiting spectrum is the superposition of the resonances of the two "frozen" enantiomeric complexes.

The analogous complex with the crotyl ligand (**3**) contains an additional element of chirality stemming from the stereogenic carbon center on the methyl-substituted terminus of the ligand. The trigonal twist, in this case, will give rise to an interconversion between diastereomers rather than enantiomers. This rearrangement, then, equilibrates (*R*)-(*C*)-**3** with (*R*)-(*A*)-**3**, and (*S*)-(*C*)-**3** with (*S*)-(*A*)-**3** (Fig. 3). The twist rearrangement does not, however, interconvert the chirality of the η^3-crotyl fragment. The (*R*) and (*S*) configuration of the crotyl moiety would probably interconvert by an η^3–η^1–η^3 process, and we have

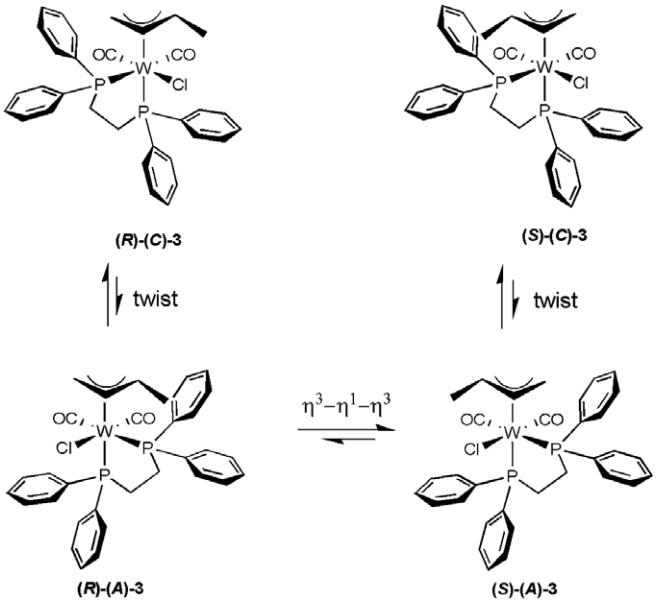

Fig. 3. Interconversion of diastereomers in **3**.

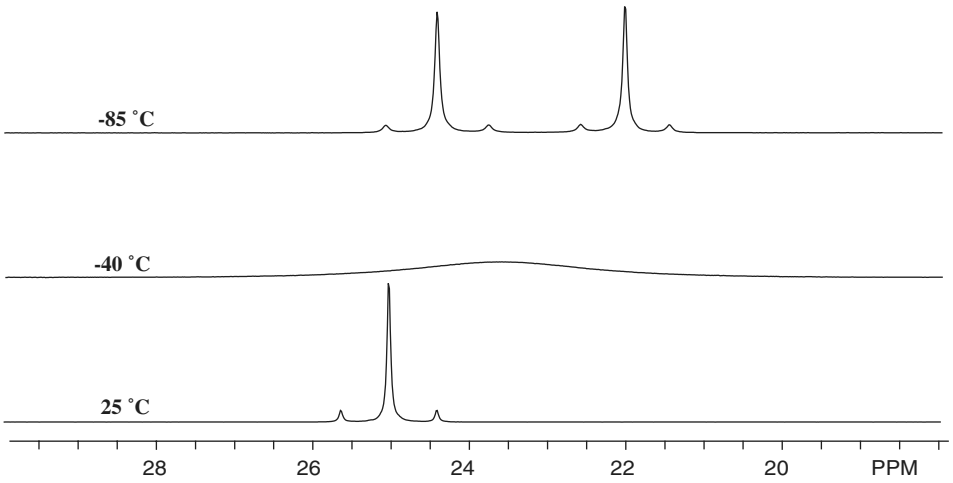

Fig. 2. Variable temperature $^{31}P\{^1H\}$ NMR of **2** in CD_2Cl_2 at 161.9 MHz.

found previously that this occurs with a comparatively large barrier for the Mo analogue **1**,which racemizes with a half-life of 1.8 h [3]. This barrier is conveniently higher for the W version **3**, which racemizes with a half-life of 4.3 h. This has important ramifications for the use of such complexes in asymmetric synthesis, since it could allow sufficient time to carry out a reaction on the crotyl fragment before it could interconvert. It should also be noted that, similarly to its Mo analogue, **3** crystallizes as a conglomerate. In both **1** and **3**, the solid state structure is that in which the equatorial P atom is *trans* to the methyl group ((*R*)-(*C*)-**3** and (*S*)-(*A*)-**3**).

An interesting feature of this spectrum is the unequal ^{183}W–^{31}P coupling to the two diastereotopic phosphorus atoms, which, since ^{183}W is only 14.3% abundant, is readily apparent from the satellite peaks. Specifically, the more downfield resonance is more strongly coupled to the metal center, and this is true for each of the tungsten crotyl complexes investigated here. This difference could in principle be useful for the assignment of the two phosphorus resonances if, for example, one supposes that these coupling constants are mainly determined by the ligand *trans* to phosphorus. A *trans* influence on one-bond metal phosphorus coupling ($^1J_{M-P}$) has been documented [23–27], in particular, the weaker bonding of a phosphine *trans* to CO has been noted to lower the magnitude of the coupling [24,25]. There is also empirical evidence relating this coupling to bond lengths; longer metal phosphorus bonds correlate with smaller coupling constants [26,28–30]. The solid state structure of **3** shows the W–P bond is longer for the phosphorus *trans* to the CO ligand (2.571 compared to 2.525 Å). On this basis, we tentatively assign the more downfield resonances in the $^{31}P\{^1H\}$ NMR spectra to the phosphorus *trans* to CO.

The low temperature $^{31}P\{^1H\}$ NMR was utilized to probe the solution dynamics. For **3**, the room temperature averaged spectrum shows two phosphorus resonances, since now the fast rearrangement does not exchange the phosphorus atoms through identical environments owing to the chirality of the η^3-crotyl ligand. In this case, a low temperature limiting spectrum would show the relative proportions of diastereomers. That is, for a given chirality of the crotyl fragment, a low temperature spectrum where the trigonal twist was slow on the NMR timescale would yield discreet resonances corresponding to the diastereomers that would result from the (*A*) and (*C*) metal chirality. (The opposite chirality in the crotyl fragment would give rise to another pair of diastereomers, though they would be enantiomers of the former pair.) Therefore, one can observe the effect of the crotyl ligand on the metal chirality by observing the ratio of isomers in a low temperature limiting spectrum.

Indeed, when a low temperature (−85 °C) $^{31}P\{^1H\}$ NMR spectrum was obtained, only two phosphorus resonances were observable (Fig. 4). Since **2** coalesces at −40 °C, it would be unlikely for **3** to be above the coalescence temperature (at the same field strength) at −85 °C, since the addition of a methyl group to an allyl terminus would not be expected to cause such a drastic change in the rearrangement barrier. Also, a study done by Whiteley *et al.* on these types of complexes with symmetrical η^3 ligands showed that the case of η^3-allyl gave the lowest barriers to the twist rearrangement [22]. The rearrangement barriers for **2** and **3** were determined from line broadening in the ^{31}P NMR spectra, and are in agreement with these findings. Specifically, for **2** the barrier of the twist rearrangement has a $\Delta G^{\neq} \approx 9.8$ kcal/mol, while in the case of **3** $\Delta G^{\neq} \approx 11.3$ kcal/mol for the conversion of the major isomer into the minor isomer. It would seem, then, that the chirality of the η^3-crotyl ligand exerts a strong influence on the metal chirality, and one diastereomer forms predominantly. Presumably, unfavorable steric interactions occur when the phosphorus in the equatorial plane is *cis* to the methyl group on the crotyl moiety, probably involving the methyl group and the phenyl rings. This would favor the configuration where the halide was *cis* to the methyl group (see Fig. 3); this is also the configuration adopted in the solid state (Fig. 5).

This notion was corroborated by low temperature $^{13}C\{^1H\}$ NMR experiments. At room temperature, the $^{13}C\{^1H\}$ NMR spectrum of **2** shows a resonance corresponding to the two CO ligands, which is a doublet with $^2J_{P-C}$ of 8.4 Hz. Here again, the additional asymmetry of **3** results in two resonances rather than one in the carbonyl region. Both of the resonances are doublets of doublets, owing to the two-bond phosphorus coupling. The notable aspect of this coupling pattern is that while one of the resonances has two coupling constants that are relatively

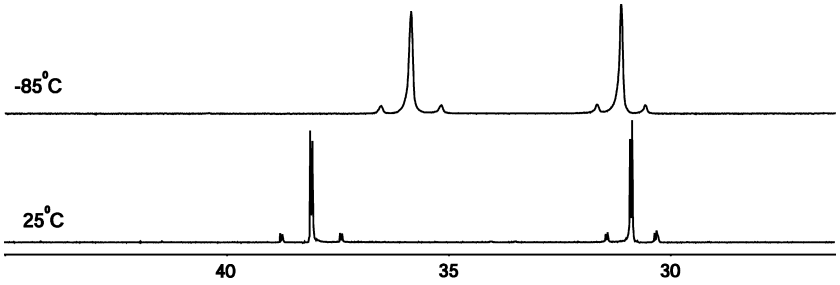

Fig. 4. Variable temperature $^{31}P\{^1H\}$ NMR of **3** in CD_2Cl_2 at 161.9 MHz.

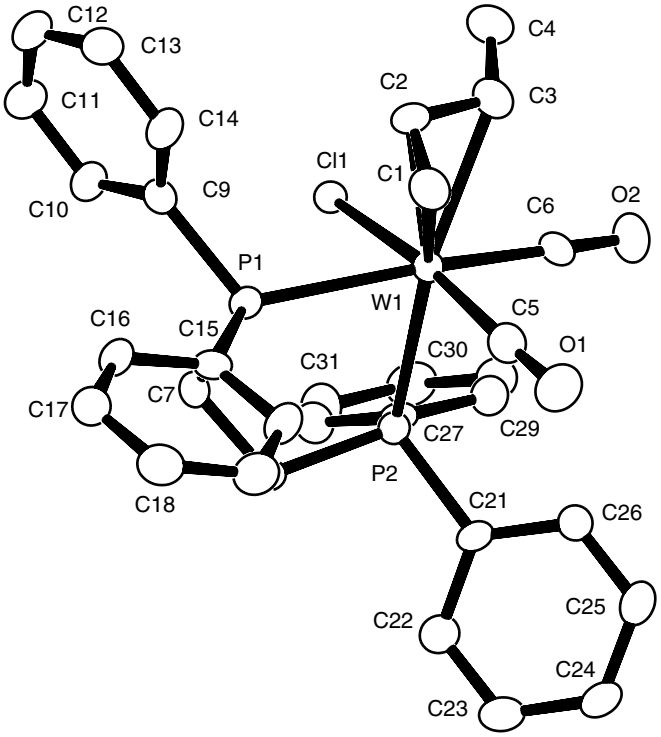

Fig. 5. ORTEP diagram of (*S*)-(*A*)-**3**.

small (4.4 Hz and 8.8 Hz), the other contains a similarly sized coupling constant as well as a much larger one (11.2 Hz and 29.8 Hz). The large coupling is indicative of a *trans* arrangement between one of the CO ligands and one of the phosphorus atoms. The large difference in the coupling patterns of the two CO resonances illustrates the fact that the average environments of these two ligands are very different. If the trigonal twist mechanism gave rise to a complete epimerization of the metal chirality, and led to a nearly equal proportion of the two diastereomers in solution, then the ^{13}C–^{31}P coupling patterns for the two CO resonances would be more symmetrical. The fact that very different coupling patterns are observed for the two CO ligands is likely due to the propensity of the chelating diphos ligand to avoid a geometry that would place it *cis* to the methyl group of the crotyl ligand.

The low temperature $^{13}C\{^1H\}$ NMR of **2** should show a similar coupling pattern to that of **3** at room temperature. However, even at −85 °C, the spectrum was still broad enough so that we were unable to obtain a spectrum of sufficient resolution to allow for an accurate determination of the ^{13}C–^{31}P coupling constants. Further cooling resulted in more broadening; it is likely that at these low temperatures another fluxional process has begun to slow to a rate that affects the lineshapes, perhaps the rotation of the phenyl rings or the interconversion of the δ and λ configurations of the backbone of diphos. Even so, while we could not determine the smaller coupling constants, it was clear again in this case that there was a larger coupling constant (~26 Hz) in one of the two resonances which would correspond to a *trans* coupling between one of the CO ligands and a phosphorus atoms.

2.2. Halide influence on syn and anti configurations

Another feature of these complexes is the possibility for *syn* and *anti* configurations of the crotyl moiety (Fig. 6). These two configurations can generally be distinguished by the examination of the coupling constants in a ^1H NMR spectrum; specifically, a central allylic proton is more strongly coupled to an *anti* proton than it is to a *syn* proton. While the coupling to an *anti* proton is usually 9–10 Hz, the *syn* coupling is only about 6–7 Hz. Therefore, by determining the coupling between the central proton and the proton on the substituted terminus, one can assign the configuration of the crotyl ligand. The *syn* configuration is favored for **3**, which exists as a 90:10 mixture of the two isomers. However, higher proportions of the *anti* isomers are observed as the size of the halide ligand increases, with especially high amounts seen in the case of iodide. For example, in the case of $W(CO)_2(\eta^3$-crotyl)(diphos)I, **4**, the synthesis initially resulted in a 73:27 mixture of isomers, with the *anti* isomer being predominant. The resonance corresponding to the proton on the substituted terminus of the major isomer is broad at room temperature owing to incomplete averaging from the twist rearrangement process, which has a higher barrier ($\Delta G^{\neq} \approx 11.9$ kcal/mol for conversion of the major *anti* isomer into the minor *anti* isomer by $^{31}P\{^1H\}$ NMR) in this case so that the *A* and *C* isomers are not yet in the fast exchange limit. A $^1H\{^{31}P\}$ NMR spectrum at elevated temperature (75 °C in C_6D_6) revealed an apparent quintet for the proton on the substituted terminus, owing to the nearly equal coupling of ~6.5 Hz to the methyl group and the central allylic proton. This smaller coupling to the central allylic proton indicates that the major isomer in **4** is that which has the *anti* crotyl configuration. In the case of **3,** the *syn* complex can be obtained as a single isomer by crystallization of the mixture. Unfortunately, though, the *syn* and *anti* isomers of **4** could not be separated in this manner, as both isomers tended to cocrystallize. A sample of enriched *syn* isomer (85%) was obtained, however, from the supernatant over the crystals. This sample was useful in that it aided in the assignment of the resonances in the low temperature NMR spectra.

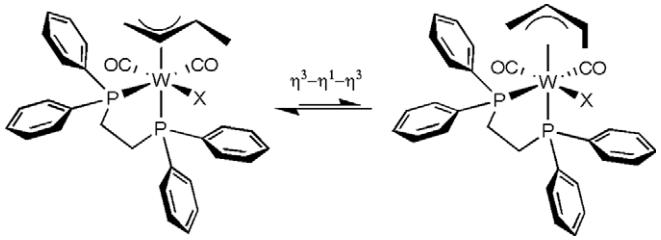

Fig. 6. *Syn* and *anti* isomers.

The variable temperature $^{31}P\{^{1}H\}$ NMR spectra (Fig. 7) of **4** revealed that, in the case of the *syn* isomer, there was once again a high preference for one of the two diastereomers, as only a single isomer was apparent even at −90 °C. The *anti* isomer, though, decoalesced into two isomers below −35 °C, with a ratio of 69:31. It appears that increasing the size of the halide results in greater repulsive steric interactions between it and the methyl group on the crotyl ligand; this is reflected in the increased fraction of *anti* isomer, which presumably lessens these unfavorable interactions. Likewise, the lower control of metal-centered chirality in the case of the *anti* isomer could be an effect of the decreased steric restrictions. If this is true, then it should be possible to obtain higher amounts of the *anti* isomer by using other unsymmetrical allyl ligands with larger alkyl substituents.

2.3. The cationic tricarbonyl analogue

The neutral complex **3** was converted to the cationic complex $[W(CO)_3(\eta^3\text{-crotyl})(\text{diphos})]SbF_6$ (**5**) with the addition of $AgSbF_6$ under an atmosphere of CO (Fig. 8). There are two possible geometries for this tricarbonyl analogue, depending on whether the CO ligands are arranged in a *facial* or a *meridional* fashion. We were unable to obtain crystals of **5** that were suitable for X-ray analysis, though the $^{13}C\{^{1}H\}$ NMR is helpful in predicting the geometry. Specifically, there are three resonances that correspond to the three inequivalent CO ligands, all of which are doublets of doublets from the coupling to the inequivalent phosphorus atoms. Two of these are in about the same region (at ~198 δ) and have similar phosphorus couplings of 4–7 Hz. The other resonance is further downfield at ~211 δ, and has larger coupling constants of 10 and 19 Hz. We attribute the large 19 Hz value to a *trans* coupling, and therefore propose the geometry that is shown in Fig. 7, since only a single CO ligand is bound *trans* to phosphorus. The intensities observed in the IR of the carbonyl stretches at 2039, 1968, and 1929 cm^{-1} with a weak

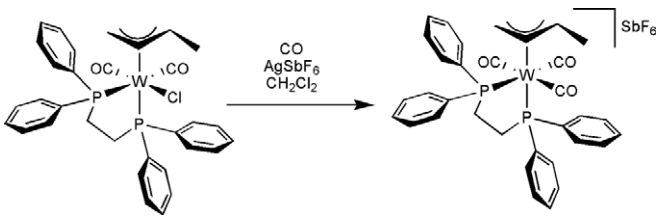

Fig. 8. Synthesis of **5**.

band at 2039 cm^{-1} are consistent with a *mer* configuration of the carbonyls.

A feature of note in the ^{1}H NMR is a large ^{31}P–^{1}H of 11.7 Hz in the resonance corresponding to the *syn* proton of the crotyl ligand. This is coupling through the metal center, and the magnitude of the coupling constant suggests that it is to the phosphorus atom bound *trans* to the crotyl. Selective decoupling of the two phosphorus resonances independently showed that it was the more downfield of the two resonances that was responsible for this coupling. As was previously mentioned, the more downfield resonance is more strongly coupled to the metal center as well. Therefore, this observation agrees with the notion that the stronger metal coupling should result from the phosphorus bound *trans* to the crotyl.

A previous study has shown that the formation of a cationic metal species greatly alters the dynamics [21]. Specifically, for the analogous cationic complex with an η^3-allyl ligand, it was shown that the trigonal twist rearrangement no longer occurs. The arrangement of the ligands about the metal is effectively rigid in the cations. The η^3 ligand is still fluxional in these complexes, although the motions are not consistent with an η^3–η^1–η^3 process. Instead, the study showed that a rotation of the allyl is occurring (Fig. 9), where the ligand oscillates between two minima oriented at 90° to each other [21].

The complex **5** no longer has metal-centered chirality, although the chirality stemming from the η^3-crotyl ligand remains. The allyl rotation does not exchange the face of

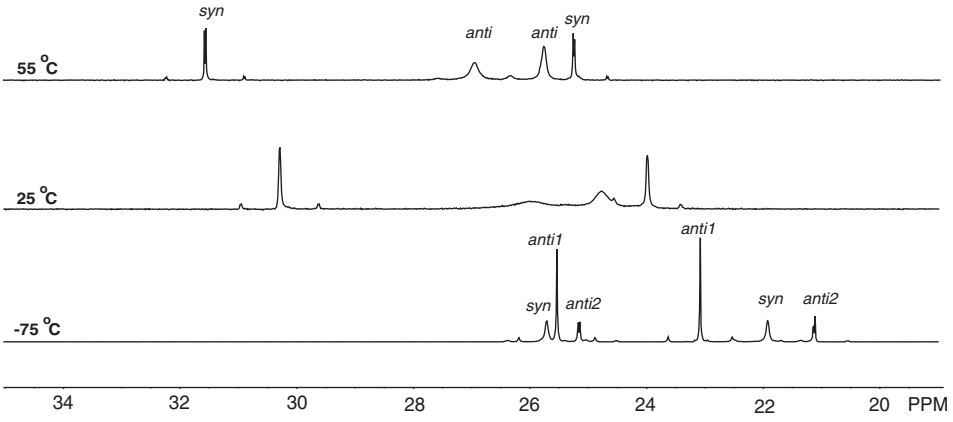

Fig. 7. Variable temperature $^{31}P\{^{1}H\}$ NMR of **4** in CD_2Cl_2 at 161.9 MHz.

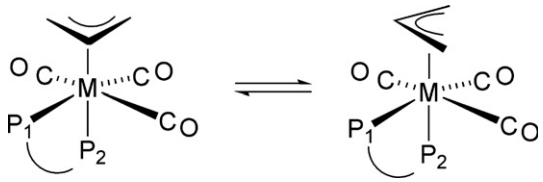

Fig. 9. Allyl rotation in cationic complexes.

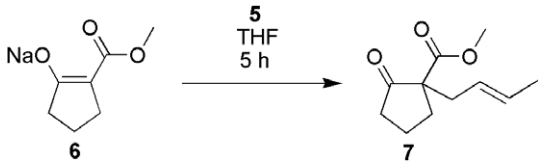

Fig. 10. Allylation with **5**.

the ligand that is bound to the metal, though, and so the ability to obtain **5** in enantiopure form would be promising in terms of use in asymmetric synthesis. This is especially true since the mechanism for racemization in the neutral analogues, the η^3–η^1–η^3 process, is comparatively slow with the cationic complexes. Optically active samples of **5** were obtained starting from amounts of **3** that were resolved by manual separation of single crystals; it was seen that the conversion of **3** into **5** occurred with retention of the chiral crotyl ligand. The decay of optical activity of **5** occurred with a half-life of ~150 h, supporting the notion that the η^3–η^1–η^3 rearrangement is greatly slowed for the cationic complex. This ensures that this process will not result in a significant loss of optical activity during the course of most reactions.

Another potentially useful feature of complex **5** is that the positive charge on the metal renders the η^3-crotyl ligand more susceptible to an attack by a nucleophile. For example, the reaction of **1** with the enolate of a β-keto ester (**6**) provides the chiral 1-but-2-enyl substituted product **7** [4]. This reaction occurs over 6 h at a temperature of 65 °C, and furnishes the product in 70% yield when PPh_3 was used as an additive. While the same reaction with the tungsten analogue **3** did not result in conversion to the desired product, we found that **5** reacts at room temperature to give **7** in less time (4 h), and with a comparable yield (77%) (Fig. 10).

When resolved **5** was used, the product was formed with 6% enantiomeric excess. It is perhaps not surprising that the selectivity of this reaction is low, since it would require the differentiation of the two faces of the prochiral nucleophile by a metal fragment where the only chiral element is the crotyl group. However, since the coordinated face of the crotyl ligand is fixed upon the formation of the cationic tricarbonyl complex, if a nucleophilic attack were to occur at the more substituted terminus, then a high enantioselectivity would be expected.

3. Conclusions

We have demonstrated that the chirality stemming from an unsymmetrical η^3-crotyl ligand can exert a strong influence on the metal chirality in pseudo-octahedral tungsten crotyl complexes that can epimerize by a low energy trigonal twist process. Variable temperature NMR experiments have indicated that there is a large preference for one of the possible isomers relative to the other. In addition, the geometry of the η^3-crotyl ligand is strongly influenced by the halide in these complexes. Specifically, the larger iodide ligand promoted a preference for the *anti* configuration. This isomeric form, which is generally disfavored with smaller halide ligands, may also exhibit new and interesting reactivity.

The conversion of the neutral species into the cationic tricarbonyl species serves to slow the η^3–η^1–η^3 rearrangement, and thus increases the racemization barrier. Also, the cationic complex was shown to be a more active allylation reagent than its neutral precursor. Future work will focus on exploring the reactivity of both neutral and cationic versions, and include the investigation of different chiral chelating ligands, with the aim of applying these complexes in asymmetric synthesis and catalysis.

4. Experimental

4.1. General

Manipulations were carried out under a nitrogen atmosphere using standard Schlenk techniques. CH_2Cl_2 was distilled over CaH under nitrogen, and THF was distilled over Na/benzophenone under nitrogen. Acetone, pentane, and Et_2O were used without drying. NMR spectra were recorded on a Bruker 400 MHz (operating at 162 MHz for ^{31}P), or a Bruker 500 MHz (operating at 126 MHz for ^{31}P). Chemical shifts are reported in ppm relative to solvent peaks (^1H, ^{13}C), or an H_3PO_4 external standard. $W(CO)_6$, NaI, NaO*t*Bu, methyl 2-oxocyclopentanecarboxylate (**6**), allyl chloride and crotyl chloride were purchased from Aldrich Chemicals; diphos and $AgSbF_6$ were purchased from Strem Chemicals.

4.2. Synthesis of tungsten complexes (*2*–*5*)

4.2.1. $W(CO)_2(\eta^3$-allyl)(diphos)Cl (*2*)

This was prepared and characterized according to a reported procedure [1].

4.2.2. syn-$W(CO)_2(\eta^3$-crotyl)(diphos)Cl (*3*)

This complex was prepared analogously to **2** with crotyl chloride being used in place of allyl chloride. A flame-dried flask equipped with a reflux condenser was charged with $W(CO)_6$ (3.64 g, 10.3 mmol) and placed under a nitrogen atmosphere. MeCN (20 mL) was added, and the solution was heated under reflux for 2 weeks, at which point it was cooled, and the solvent removed under vacuum. To

the solid was added THF (20 mL) under a nitrogen atmosphere, followed by crotyl chloride (1.25 mL, 15.3 mmol), and the resulting mix was heated at 60 °C for 1 h. Diphos (4.10 g, 10.3 mmol) was added to the hot solution, which was then allowed to cool slowly to room temperature. The solvent was removed under vacuum, and the crude mixture was passed through a column of silica gel eluting with CH_2Cl_2 (5.50 g, 73%). The product was formed in a 90/10 mixture of *syn*/*anti* isomers; pure *syn*-**3** could be obtained by crystallizing from CH_2Cl_2/Et_2O. Anal. Calc. for $C_{32}H_{31}ClO_2P_2W$: C, 52.73; H, 4.29; Found: C, 52.71; H, 4.35%. IR (CH_2Cl_2): ν(CO) 1916, 1835 cm^{-1}. ^1H NMR (400 MHz, $CDCl_3$, δ): 7.80–7.20 (20H, m, aromatics), 3.15 (1H, m, $J_{syn'/central} = 6.1$ Hz, $J_{syn'/anti} = 2.0$ Hz, $H_{syn'}$), 3.02 (1H, m, $H_{central}$), 3.02–2.78 (2H, m, PCH_2CH_2P), 2.64 (1H, m, $J_{anti/central} = 10.1$ Hz, $J_{anti/Me} = 6.3$ Hz, H_{anti}), 2.39–1.96 (2H, m, PCH_2CH_2P), 1.86 (3H, d, $J_{Me/anti} = 6.3$ Hz, CH_3), 1.48 (1H, d, $J_{anti'/central} = 9.1$ Hz, $J_{anti'/syn} = 2.0$ Hz, $H_{anti'}$). $^{13}C\{^1H\}$ NMR (125.8 MHz, CD_2Cl_2, δ): 217.8 (dd, *C*O, $J_{P-C} = 11.2$, 29.8 Hz), 216.2 (dd, *C*O, $J_{P-C} = 4.4$, 8.8 Hz), 135.1–128.3 (aromatics), 78.3 (d, η^3-crotyl, $J_{P-C} = 3.1$ Hz), 78.2 (d, η^3-crotyl, $J_{P-C} = 3.3$ Hz), 42.7 (s, η^3-crotyl), 27.7 (dd, PCH_2CH_2P, $J_{P-C} = 11.4$, 27.5 Hz), 24.9 (dd, PCH_2CH_2P, $J_{P-C} = 12.7$, 27.5 Hz), 16.1 (s, CH_3). ^{31}P NMR (161.9 MHz, CD_2Cl_2, δ): 38.1 (d, $J_{P-P} = 7.3$ Hz, $J_{W-P} = 218$ Hz), 30.9, (d, $J_{P-P} = 7.3$ Hz, $J_{W-P} = 178$ Hz). $[\alpha]_{365}$ ($c = 2.024 \times 10^{-4}$, CH_2Cl_2): 430°. The allylic coupling constants were determined with a $^1H\{^{31}P\}$ NMR experiment.

4.2.3. $W(CO)_2(\eta^3$-crotyl)(diphos)I (**4**)

A flame-dried flask equipped with a reflux condenser was charged with 300 mg (0.412 mmol) of **3** and 5.0 g (33 mmol) of NaI, and was evacuated and backfilled with nitrogen. Acetone (5 mL, degassed with a freeze/pump thaw cycle) was then added, and the resulting mixture was heated under reflux for 24 h, at which point the mixture was cooled, and the solvent was removed under vacuum. The product was then taken up in CH_2Cl_2 and filtered through Celite to remove the sodium salt. Evaporation of the solvent resulted in a 73/27 mixture of *anti* and *syn* isomers. Crystals were obtained by slow diffusion of Et_2O or pentane into a CH_2Cl_2 solution (141 mg, 42%). Anal. Calc. for $C_{32}H_{31}IO_2P_2W$: C, 46.85; H, 3.81; Found: C, 46.83; H, 3.83%. IR (CH_2Cl_2): ν(CO) 1926, 1838 cm^{-1}. *Anti*; ^1H NMR (400 MHz, $CDCl_3$, δ): 7.80–7.20 (20H, m, aromatics), 4.47 (1H, br, H_{syn}), 3.71 (1H, m, $H_{syn'}$), 3.47 (1H, m, $H_{central}$), 3.21–3.08 (2H, m, PCH_2CH_2P), 2.50–2.15 (2H, m, PCH_2CH_2P), 2.28 (1H, br d, $H_{anti'}$), 1.35 (3H, d, $J_{Me/syn} = 6.4$ Hz, CH_3), $^{31}P\{^1H\}$ NMR (161.9 MHz, CD_2Cl_2, δ): 25.9 (br), 24.7 (br). *Syn*; ^1H NMR (400 MHz, $CDCl_3$, δ): 7.81–7.31 (20H, m, aromatics), 3.70 (1H, m, $H_{central}$), 3.23 (1H, m, $H_{syn'}$), 3.37–3.02 (2H, m, PCH_2CH_2P), 2.60 (1H, m, H_{anti}), 2.68–2.18 (2H, m, PCH_2CH_2P), 2.21 (3H, d, $J_{Me/anti} = 6.4$ Hz, CH_3), 1.51 (1H, dd, $J_{anti'/central} = 9.6$ Hz, $J_{anti'/syn} = 2.0$ Hz, $H_{anti'}$), $^{31}P\{^1H\}$ NMR (161.9 MHz, CD_2Cl_2, δ): 30.1 (s, $J_{W-P} = 216$ Hz), 23.9 (s, $J_{W-P} = 186$ Hz).

The allylic coupling constants were determined with a $^1H\{^{31}P\}$ NMR experiment at 75 °C in C_6D_6. ^1H NMR (400 MHz, C_6D_6, 75 °C, δ): *Anti*; 7.82–6.95 (20H, m, aromatics), 4.65 (1H, dq, $J_{syn/central} = 6.5$, $J_{syn/Me} = 6.5$, H_{syn}), 3.82 (1H, dd, $J_{syn'/central} = 6.8$, $J_{syn'/anti} = 1.5$ Hz, $H_{syn'}$), 3.72 (1H, m, $H_{central}$), 3.05–2.85 (2H, m, PCH_2CH_2P), 2.36 (1H,dd, $J_{anti'/central} = 10.2$ Hz, $J_{anti'/syn} = 1.5$, $H_{anti'}$), 2.17–2.00 (2H, m, PCH_2CH_2P), 1.37 (3H, d, $J_{Me/syn} = 6.5$ Hz, CH_3). *Syn*; 7.94–6.95 (20H, m, aromatics), 3.73 (1H, m, $H_{central}$), 3.25 (1H, dd, $J_{syn'/central} = 6.4$, $J_{syn'/anti} = 2.0$, $H_{syn'}$), 3.18 (1H, ddd, $J = 14.0$, 10.0, 7.2 Hz, PCH_2CH_2P), 2.90 (1H, ddd, *anti* isomer is superimposed, PCH_2CH_2P), 2.60 (1H, dq, $J_{anti/central} = 10.2$ Hz, $J_{anti/Me} = 6.4$ Hz, H_{anti}), 2.30–2.00 (2H, m, PCH_2CH_2P), 2.28 (3H, d, $J_{Me/anti} = 6.4$ Hz, CH_3), 1.56 (1H, dd, $J_{anti'/central} = 8.9$ Hz, $J_{anti'/syn} = 2.0$ Hz, $H_{anti'}$).

4.2.4. [syn-$W(CO)_3(\eta^3$-crotyl)(diphos)]SbF_6 (**5**)

A three-necked flask was charged with **3** (108 mg, 0.148 mmol), and was purged with CO gas. CH_2Cl_2 (5 mL) was then added, followed by $AgSbF_6$ (51 mg, 0.148 mmol) under a stream of CO. The mixture was stirred for 1 h, and then filtered through Celite. The solvent was removed under vacuum, resulting in a yellow solid. Crystals were obtained by diffusion of Et_2O into a CH_2Cl_2 solution of the product (121 mg, 85%). Anal. Calc. for $C_{33}H_{31}F_6O_3P_2SbW \cdot H_2O$: C, 40.65; H, 3.41; Found: C, 40.42; H, 3.20%. IR (CH_2Cl_2): ν(CO) 2039 (w), 1968 (m), 1929 (s) cm^{-1}. ^1H NMR (500 MHz, CD_2Cl_2, δ): 7.73–7.18 (20H, m, aromatics), 4.94 (1H, ddd, $J_{central/anti'} = 10.8$, $J_{central/anti} = 10.5$ Hz, $J_{central/syn'} = 7.0$ Hz, $H_{central}$), 3.25 (1H, dd, $J_{P-H} = 11.7$ Hz, $J_{syn'/central} = 7.0$ Hz, $H_{syn'}$), 3.13 (1H, dq, $J_{anti/central} = 10.5$ Hz, $J_{anti/Me} = 6.0$ Hz, H_{anti}), 3.07–2.72 (4H, m, PCH_2CH_2), 2.17 (1H, d, $J_{anti'/central} = 10.8$ Hz, $H_{anti'}$), 2.12 (3H, d, $J_{Me/anti} = 6.0$ Hz, CH_3), $^{13}C\{^1H\}$ NMR (125.7 MHz, CD_2Cl_2, δ): 211.1 (dd, *C*O, $J_{P-C} = 10.0$, 19.2 Hz), 198.3 (dd, *C*O, $J_{P-C} = 7.3$, 6.0 Hz), 198.1 (t, *C*O, $J_{P-C} = 4.5$ Hz), 132.6–129.2 (aromatics), 92.8 (s, η^3-crotyl), 64.6 (η^3-crotyl), 48.3 (s, η^3-crotyl), 29.5 (dd, PCH_2CH_2P, $J_{P-C} = 13.6$, 32.4 Hz), 29.2 (dd, PCH_2CH_2P, $J_{P-C} = 11.6$, 31.7 Hz), 19.1 (s, CH_3), ^{31}P NMR (202.4 MHz, $CDCl_3$, δ): 42.9 (d, $J_{P-P} = 19.7$ Hz, $J_{W-P} = 213$ Hz), 39.8 (d, $J_{P-P} = 19.7$ Hz, $J_{W-P} = 199$ Hz).

4.3. Allylic alkylation reaction

Methyl-2-oxocyclopentanecarboxylate (40 μL, 0.32 mmol) was added to a slurry of NaO*t*Bu (27.4 mg, 0.286 mmol) in THF (5 mL) under a nitrogen atmosphere. The mixture was stirred for 5 min, at which point **5** (140 mg, 0.146 mmol) was added as a solution in THF (3 mL). The resulting mixture was stirred for 4 h, and was then diluted with Et_2O (10 mL) and washed with 10% KOH solution (2 × 10 mL). The organic portion was washed with 10% HCl (10 mL), and then brine (10 mL), and dried over

Table 1
Crystallographic data for (*S*)-(*A*)-**3**

	(*S*)-(*A*)-**3**
Color, shape	Red block
Empirical formula	$C_{32}H_{31}ClO_2P_2W$
Formula weight	728.85
Radiation (Å)	Mo Kα (monochr.) 0.71073
T (K)	173
Crystal system	Monoclinic
Space group	$P2_12_12_1$ (No. 19)
Unit cell dimensions	
a (Å)	11.6499(4)
b (Å)	13.2044(3)
c (Å)	18.4470(6)
V (Å^3)	2837.70(13)
Z	4
D_{calc} (g cm^{-3})	1.706
μ (cm^{-1}) (Mo Kα)	43.11
Crystal size (mm)	$0.07 \times 0.07 \times 0.10$
Reflcns Tot., unique, used[a]	6008, 3642; 5395
R_{int}	0.0549
Parameters, restraints	172, 0
R_1[a], wR_2[b], GOF	0.0328, 0.028, 1.29
Resid. density (e Å^{-3})	−1.07 < 0.68

[a] $R_1 = \sum \|F_o| - |F_c\| / \sum |F_o|$, for all $I > 3\sigma(I)$.

[b] $wR_2 = \left[\sum[w(F_o^2 - F_c^2)^2] \Big/ \sum[w(F_o^2)^2]\right]^{1/2}$.

$MgSO_4$. The solvent was removed under vacuum, and the residue was purified on silica gel eluting with 3:1 hexanes:Et_2O. Yield: 16 mg (77%). The enantiomeric excess was determined with the use of (+)-Eu(hfc)$_3$ as a chiral shift agent in $CDCl_3$; it was observed the resonance corresponding to the methoxy group on **7** was split after a downfield shift of ~0.5 δ.

4.4. Crystal structure determination and refinement

Data were collected on a Nonius KappaCCD (Mo Kα radiation) diffractometer and scaled using HKL2000 [31,32]. The data were not specifically corrected for absorption other than the inherent corrections provided by Scalepack [32]. The structures were solved by direct methods (SIR92) and refined on *F* for all reflections [33,34]. Non-hydrogen atoms were refined with anisotropic displacement parameters. Hydrogen atoms were included at calculated positions. Relevant crystal and data parameters are presented in Table 1.

The chloride derivative **3** crystallized as a conglomerate in the orthorhombic space group $P2_12_12_1$ consistent with the observed absences. The particular crystal chosen was cut to provide a sample for optical rotation determination and the remaining portion used for X-ray structure determination had a (*S*)-(*A*) configuration for which the absolute configuration was determined by inversion of coordinates ($R = 2.81$, $R_w = 2.78$ compared to $R = 5.56$, $R_w = 6.30$).

The iodide crystallized as a conglomerate in the monoclinic space group $P2_1$. The complex was predominantly the anti isomer, but there was a disorder between a carbonyl and crotyl resulting in (*R*)-(*C*) and (*S*)-(*A*) configurations in the solid (ratio ~ 2:1) that did not provide a structure with reliable metrical data.

Appendix A. Supplementary material

Tables of crystallographic data parameters, bond lengths and angles for (*S*)-(*A*)-W(CO)$_2$(η^3-crotyl)-(diphos)Cl. CCDC <612693> contains the supplementary crystallographic data for <**3**>. These data can be obtained free of charge via http://www.ccdc.cam.ac.uk/conts/retrieving.html, or from the Cambridge Crystallographic Data Centre, 12 Union Road, Cambridge CB2 1EZ, UK; fax: (+44) 1223-336-033; or e-mail: deposit@ccdc.cam.ac.uk. Supplementary data associated with this article can be found, in the online version, at doi:10.1016/j.jorganchem.2006.07.037.

References

[1] J.W. Faller, D.A. Haitko, R.D. Adams, D.F. Chodosh, J. Am. Chem. Soc. 99 (1977) 1654.
[2] J.W. Faller, D.A. Haitko, R.D. Adams, D.F. Chodosh, J. Am. Chem. Soc. 101 (1979) 865.
[3] J.W. Faller, N. Sarantopoulos, Cryst. Growth Des. 5 (2005) 2356.
[4] B.M. Trost, M. Lautens, Tetrahedron 43 (1987) 4817.
[5] B.M. Trost, M. Lautens, J. Am. Chem. Soc. 104 (1982) 5543.
[6] J.W. Faller, C. Lambert, Tetrahedron 41 (1985) 5755.
[7] B.M. Trost, M. Lautens, J. Am. Chem. Soc. 109 (1987) 1469.
[8] R.H. Yu, J.S. McCallum, L.S. Liebeskind, Organometallics 13 (1994) 1476.
[9] I. Shimizu, T. Sakamoto, S. Kawaragi, Y. Maruyama, A. Yamamoto, Chem. Lett. (1997) 137.
[10] B.M. Trost, I. Hachiya, J. Am. Chem. Soc. 120 (1998) 1104.
[11] A.V. Malkov, I.R. Baxendale, D. Dvorak, D.J. Mansfield, P. Kocovsky, J. Org. Chem. 64 (1999) 2737.
[12] F. Glorius, A. Pfaltz, Org. Lett. 1 (1999) 141.
[13] F. Glorius, M. Neuburger, A. Pfaltz, Helv. Chim. Acta 84 (2001) 3178.
[14] M. Palucki, J.M. Um, D.A. Conlon, N. Yasuda, D.L. Hughes, B. Mao, J. Wang, P.J. Reider, Adv. Synth. Catal. 343 (2001) 46.
[15] O. Belda, C. Moberg, Acc. Chem. Res. 37 (2004) 159.
[16] B.M. Trost, M.H. Hung, J. Am. Chem. Soc. 105 (1983) 7757.
[17] G.C. Lloyd-Jones, A. Pfaltz, Angew. Chem., Int. Ed. 34 (1995) 462.
[18] J. Lehmann, G.C. Lloyd-Jones, Tetrahedron 51 (1995) 8863.
[19] H. Frisell, B. Akermark, Organometallics 14 (1995) 561.
[20] R. Pretot, G.C. Lloyd-Jones, A. Pfaltz (Eds.), Pure Appl. Chem. 70 (1998) 1035.
[21] J.W. Faller, D.A. Haitko, J. Organometal. Chem. 149 (1978) C19.
[22] J. Friend, S.Y. Master, I. Preece, D.M. Spencer, K.J. Taylor, A. To, J. Waters, M.W. Whiteley, J. Organometal. Chem. 645 (2002) 218.
[23] S.O. Grim, R.L. Keiter, W. McFarlan, Inorg. Chem. 6 (1967) 1133.
[24] S.O. Grim, Da. Wheatlan, Inorg. Chem. 8 (1969) 1716.
[25] G.G. Mather, A. Pidcock, J. Chem. Soc. A—Inorg. Phys. Theor. (1970) 1226.
[26] R. Mason, D.W. Meek, Angew. Chem., Int. Ed. 17 (1978) 183.
[27] G.G. Mather, G.J.N. Rapsey, A. Pidcock, Inorg. Nucl. Chem. Lett. 9 (1973) 567.
[28] H.J. Plastas, J.M. Stewart, S.O. Grim, Inorg. Chem. 12 (1973) 265.
[29] G.G. Mather, A. Pidcock, G.J.N. Rapsey, J. Chem. Soc. Dalton Trans. (1973) 2095.

[30] R. Mason, L. Randacci, J. Chem. Soc. A—Inorg. Phys. Theor. (1971) 1150.
[31] W. Minor, Z. Otwinowski (Eds.), HKL2000 (Denzo-SMN) Software Package. Processing of X-ray Diffraction Data Collected in Oscillation Mode, Methods in Enzymology, Macromolecular Crystallography, Academic Press, New York, 1997.
[32] Z. Otwinowski, W. Minor, in: International Tables for Crystallography, E. Arnold (Ed.), vol. F, Kluwer Academic Press, Dordrecht, 2001.
[33] Texsan, TEXSAN for Windows version 1.06: Crystal Structure Analysis Package, Molecular Structure Corporation (1997–9), 1999.
[34] G. Altomare, C. Cascarano, A. Giacovazzo, J. Guagliardi, Appl. Crystallogr. 26 (1993) 343.